Brain MR: Pathologic Correlation with Gross and Histopathology. 1. Lacunar Infarction and Virchow-Robin Spaces

Bruce H. Braffman, Robert A. Zimmerman, John Q. Trojanowski, Nicholas K. Gonatas, William F. Hickey and William W. Schlaepfer

AJNR Am J Neuroradiol 1988, 9 (4) 621-628
http://www.ajnr.org/content/9/4/621

Brain MR: Pathologic Correlation with Gross and Histopathology.
1. Lacunar Infarction and Virchow-Robin Spaces

Bruce H. Braffman[1, 2]
Robert A. Zimmerman[1]
John Q. Trojanowski[3]
Nicholas K. Gonatas[3]
William F. Hickey[3]
William W. Schlaepfer[3]

MR imaging was performed on 36 formalin-fixed brain specimens. For three of these specimens, in vivo MR studies had also been performed before death. Changes that take place in the MR appearance of the brain after fixation are discussed. Gross and microscopic pathology revealed 14 lacunar infarctions in seven cases and enlarged Virchow-Robin spaces (état criblé) in four. Both types of lesion were seen in specimens from predominantly elderly, hypertensive patients. Eight lacunae were in the deep gray-matter nuclei (four in the putamen with variable involvement of the internal capsule and caudate nuclei, two in the thalami, and two in the dentate nuclei), five were in the supratentorial white matter, and one was in the brainstem. Enlarged Virchow-Robin spaces were identified in the basal ganglia. All lesions were detected on MR. CT failed to disclose the brainstem and dentate lacunae and the enlarged Virchow-Robin spaces. On MR, all lacunae were slitlike or ovoid, except one that was round. They were less than 1 cm in greatest diameter in all but two cases. The lacunae were hyperintense relative to brain parenchyma on both long TR sequences (short and long TEs) in all cases except that of a chronic infarct that underwent cystic change and was isointense relative to CSF on all pulse sequences. In contrast, dilated Virchow-Robin spaces were isointense relative to CSF in vivo or to fluid in the subarachnoid space in the postmortem state on all pulse sequences in all four cases. They were round or linear, and in general were smaller than the lacunae, although some overlap in size did occur. They were seen at the level immediately above the bifurcation of the internal carotid into the middle and anterior cerebral arteries and were seen on successive axial sections in the putamen (most prominent along its lateral margin) and in the internal capsule.

MR studies of gross and microscopic pathology of lacunae and dilated Virchow-Robin spaces are useful in correlating MR and pathologic findings. However, changes resulting from the fixation process must be considered when postmortem and in vivo MR findings are correlated.

This article appears in the July/August 1988 issue of *AJNR* and the September 1988 issue of *AJR*.

Received September 8, 1987; accepted after revision February 24, 1988.

Presented at the annual meeting of the American Society of Neuroradiology, New York City, May 1987.

This work was supported in part by National Institutes of Health grant PO1-AG06107.

[1] Department of Radiology, Hospital of the University of Pennsylvania, 3400 Spruce St., Philadelphia, PA 19104. Address reprint requests to R. A. Zimmerman.

[2] Department of Radiology, Memorial Hospital, Hollywood, FL 33021.

[3] Division of Neuropathology, Hospital of the University of Pennsylvania, Philadelphia, PA 19104.

***AJNR* 9:621–628, July/August 1988**
0195-6108/88/0904-0621

The perivascular space, known as the Virchow-Robin space, is an invagination of the subarachnoid space that surrounds the vessel wall as it courses from the subarachnoid space through the brain parenchyma [1]. It surrounds the arteries, arterioles, veins, and venules, but not the capillaries, of the CNS. In état criblé (riddled with shot- or sievelike perforations), first described by Durand-Fardel [2], these perivascular spaces are dilated [1–5]. They may occur in the basal ganglia or in the white matter. Associated parenchymal changes surrounding the dilated perivascular spaces may or may not be present. Fisher [4] stated there is no apparent alteration of the adjacent tissue. Brierly and Graham [5] described a narrow border of fibrillary gliosis surrounding the cavity. Blackwood [3] observed thin, pale, and sinuous myelin sheaths in the parenchyma that surrounds the vessel.

Durand-Fardel [2] was also the first to use the term *lacuna* (cavity). Fisher [4, 6] defined *lacunes* as infarctions caused by perforating branch occlusion that may occur in both the central gray-matter nuclei and white matter. État lacunaire, first described by Marie [7], is a state of multiple lacunar infarctions [7]. In Marie's initial description, it was associated with the clinical features of dementia and pseudobulbar palsy. However, Fisher [4] rarely observed this clinical correlation in subjects with multiple lacunae.

Awad et al. [8] found état criblé accounted for many incidental subcortical lesions identified on MR imaging in the elderly. In this study, MR features of état criblé and lacunar infarctions are correlated with gross and histopathology.

Materials and Methods

We prospectively performed MR examinations on 36 brain specimens. Thirty-three were examined after fixation of brain tissue for 1–2 weeks with 4% neutral buffered formalin, and three were studied both within 2 months before death and after death and subsequent formalin fixation of the brain. One patient was only investigated 10 weeks before death. Before MR imaging, the brain specimens were removed from the formalin solution and placed in water for 12–48 hr. The resultant solution was mostly water with a very dilute amount of formalin. After imaging, the specimens were replaced in the fixative.

The patients whose brains were examined were 30–94 years old (mean, 62.6 years); 19 were male and 18 were female; 24 were 60 years old or older. Included were patients both with and without known neurologic symptoms during life. All studies were performed with a 1.5-T GE Signa unit with spin-echo (SE) multisection imaging sequences. Short TR sequences, 300, 600/20 (TR/TE), were obtained in the sagittal or axial planes; long TR sequences, 2500/20 or 30 (first echo), 80 (second echo), were obtained in the coronal and axial planes. All scans were obtained with a 5-mm slice thickness and a 2.5-mm slice gap. The matrix size was 256 × 128.

CT scans were obtained in 20 of the 36 cases within 3 months before death. All CT studies were performed on a GE 9800 scanner. We correlated the MR and CT examinations in all available cases.

After a minimum of 2 weeks of fixation, one of four neuropathologists sliced the brain into sections ranging from approximately 3 mm to 1 cm. One or both neuroradiologists attended each gross pathologic examination to enable direct correlation between MR findings and gross pathology. Representative foci of abnormalities were photographed. Microscopic sections of lesions were obtained and stained with H and E, and when appropriate with Weil, Luxol Fast Blue, and/or Bodian stains. Histopathologic analysis was conducted by one of four neuropathologists with light microscopy. All studies, pathology and imaging, were reviewed jointly by both neuroradiologists and a neuropathologist.

Results

Basal Ganglia and Thalamus

Six lesions in the basal ganglia and thalamus in four cases (cases 1–4) were lacunar infarctions (Table 1). Three were

TABLE 1: Lacunar Infarctions and Basal Ganglia État Criblé

Type of Lesion: Case No.	Age	Gender	Cardiovascular Status			MR and Pathologic Features		Approximate Size (mm)
			HTN	Other	Systemic Atherosclerosis	Site	Morphology	
Lacuner infarctions:								
1	37	F	No	No	Minimal	(1) L Caudate internal capsule, putamen	Slitlike	8 × 2
						(2) R putamen	Slitlike	4 × 2
						(3) Bilateral dentate	Slitlike	5 × 3 3 × 3
2	78	M	Yes (P + C)	No	Severe	L internal capsule & putamen	Partly slitlike & partly ovoid	10 × 2
3	73	F	Yes (P + C)	No	Severe	(1) Bilateral thalamic	Slitlike	5 × 1 4 × 1
						(2) Brainstem	Slitlike	3 × 1
4	71	F	Yes (C)	DM	No	L putamen	Round	14 × 13
5	78	F	Yes (P + C)	MI	Severe	R centrum semiovale near entrance to internal capsule	Slitlike	4 × 2
6	70	F	Yes (P + C)	MI, A	Severe	Bifrontal white matter (four lesions)	Ovoid	2 × 2 (all)
État criblé in the basal ganglia:								
4	71	F	Yes (C)	DM	No	Putamen and internal capsule	Round or linear	1 × 1 to 3 × 1 (in vivo); 1 × 1 to 4 × 2 (postmortem)
7	75	M	Yes (P)	Smoker	Severe	Putamen and internal capsule	Round or linear	2 × 2 to 1 × 1
8	57	M	Yes (P + C)	No	Severe	Putamen and internal capsule	Round or linear	3 × 1 to 1 × 1
9	51	M	Yes (P + C)	No	Severe	Putamen and internal capsule	Round or linear	3 × 2 to 1 × 1

Note.—HTN = hypertension; L = left; R = right; P = pathologic evidence of hypertension (concentric left ventricular hypertrophy); C = clinical evidence of hypertension during life; DM = diabetes mellitus; MI = post-myocardial infarction; A = arrythmia.

from patients 50 years old or older and had clinical and/or pathologic (i.e., concentric muscular hypertrophy of the left ventricle) evidence of hypertension. One subject was 37 years old and was not hypertensive. The lacunae involved the putamen and internal capsule in one case; the putamen, internal capsule, and caudate nucleus in one; the putamen alone in two; and the bilateral thalami in one. On MR, four lacunae were slitlike (Fig. 1), one was partly slitlike and partly ovoid (Fig. 2), and one was round (Fig. 3). They ranged in size from approximately 3 × 1 to 14 × 13 mm. CT scans revealed corresponding hypodensities (Figs. 1C and 2C). Gross pathologic evaluation confirmed the morphologic features that were demonstrated on MR or CT (Figs. 1F and 3H), and histopathology confirmed the diagnoses of lacunar infarctions.

In four subjects 50 years old or older (cases 4 and 7–9), all with clinical and/or pathologic evidence of hypertension, perforations of état criblé were identified in the putamen and internal capsule (Table 1). On MR (Figs. 3A–3G) they were minute (approximate measurements ranging from 1 × 1 to 2 × 5 mm in greatest diameter) and were round or linear in morphology. They began at the level of the bifurcation of the internal carotid artery into the anterior and middle cerebral arteries and extended a variable distance on successive axial sections through the thickness of the putamen and were particularly noticeable along the lateral margin of the putamen (Fig. 3I). They were slightly more prominent in size after formalin fixation (Figs. 3A–3G and Table 1). CT was performed in two cases and failed to reveal any abnormality.

Posterior Fossa

Three lesions in the posterior fossa in two cases (cases 1 and 3) were lacunar infarctions, two in the dentate nuclei and one in the brainstem (Table 1). One subject had been hypertensive and elderly; the other was normotensive and 37 years old. All lacunae were slitlike on MR (Figs. 4 and 5). CT failed to reveal any of these lesions, which ranged in size from approximately 3 × 1 to 5 × 3 mm. Gross pathologic exami-

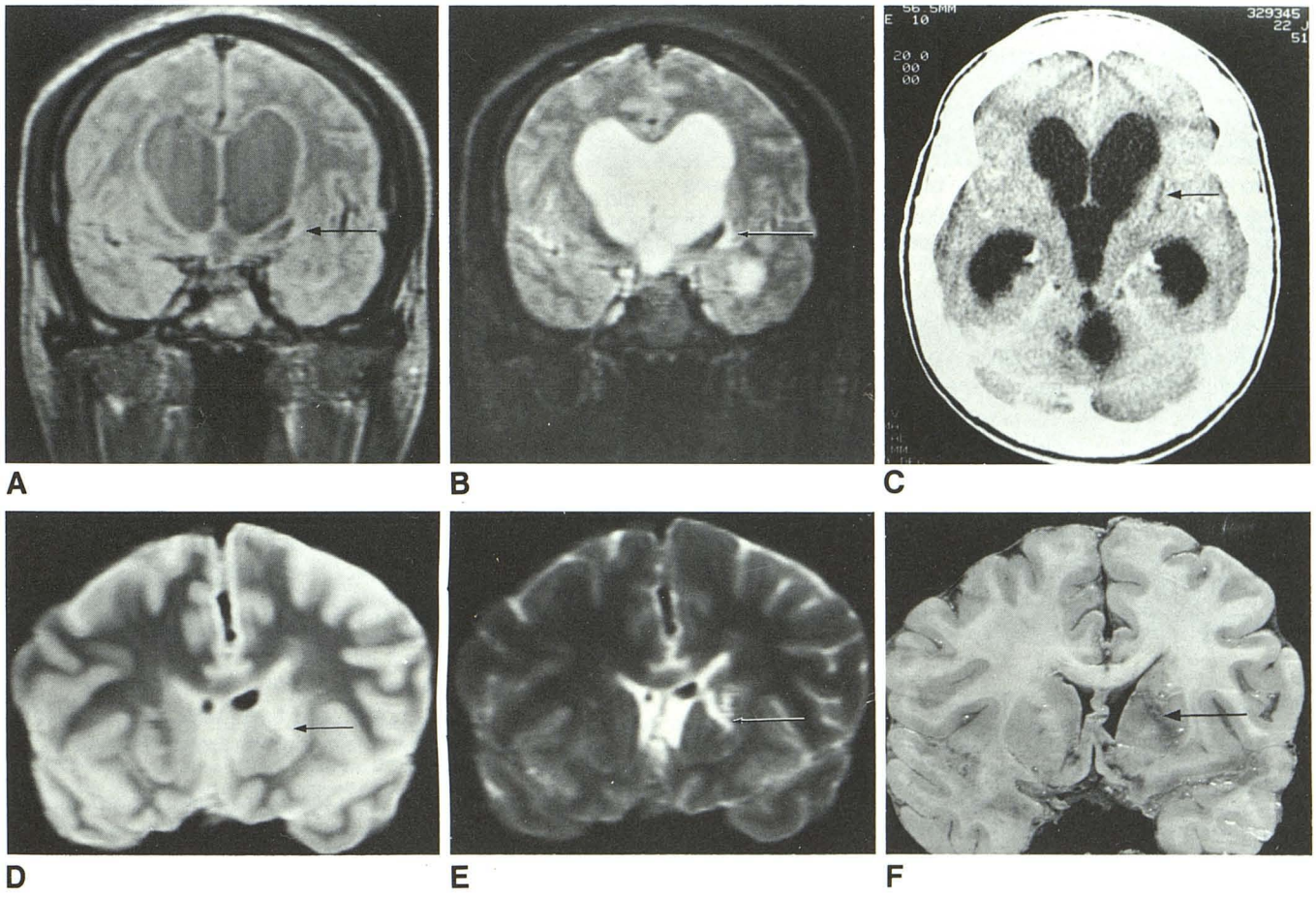

Fig. 1.—Case 1: left basal ganglia lacunar infarction (*arrows*). (A smaller, contralateral putaminal lacuna is not shown here.)

***A* and *B*, Coronal MR images, 2500/30 (*A*) and 2500/80 (*B*), prior to death. Slitlike lacuna is hyperintense relative to brain parenchyma on both long TR sequences. On long TR/short TE sequence (*A*), lacuna is also hyperintense relative to CSF.**

***C*, Axial CT scan. Left slitlike hypodensity is present.**

***D* and *E*, Coronal MR images, 2500/30 (*D*) and 2500/80 (*E*), after death and subsequent formalin fixation of brain. Compared with MR studies before death, orientation of left lacuna has changed, likely because of decompression of ventricles. Morphology and intensity relative to brain parenchyma of lacuna have not changed. Note, however, that water mixed with dilute formalin is hyperintense relative to brain parenchyma on long TR/short TE sequence (*D*), while CSF is hypointense (*A*).**

***F*, Gross pathology. Slitlike, irregular cavity in left basal ganglia transects head of caudate nucleus, anterior limb of internal capsule, and putamen.**

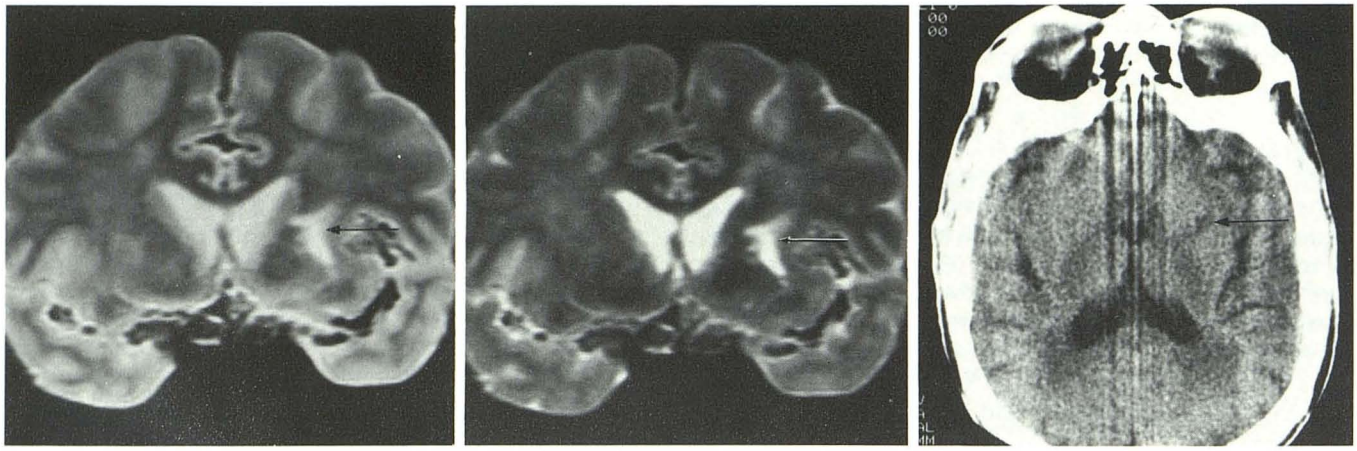

Fig. 2.—Case 2: lacunar infarct (*arrows*) in left putamen and internal capsule.
***A* and *B*, Coronal MR images, 2500/30 (*A*) and 2500/80 (*B*), of brain specimen. Partly ovoid and slitlike lacunar infarct is hyperintense relative to brain parenchyma on both long TR sequences.**
***C*, Axial CT scan. Lacuna is ovoid and slitlike hypodensity.**

nation displayed slitlike cavities, and histopathologic evaluation confirmed lacunar infarctions.

Supratentorial White Matter

Five lesions in the white matter in two cases (Table 1, cases 5 and 6) were infarctions with varying amounts of cavitation. Both were from hypertensive and elderly patients. On MR the one lesion in case 5 was slitlike (see Fig. 1 in our companion article [9]), and the four lesions in case 6 were ovoid. Their approximate sizes ranged from 2 × 2 to 4 × 2 mm. CT was performed in case 5 and revealed a linear hypodensity. On gross pathologic examination, the lesion in case 5 was a slitlike cavity, and no gross abnormality was observed in the four lesions in case 6. Histopathology confirmed the diagnosis of infarction in all five lesions.

The relative MR signal intensities of the noncystic lacunae (Figs. 1, 2, 4, and 5) are listed in Table 2 (cases 1–3, 5, and 6). The intensities of the cystic lacunar infarct (Figs. 3) and of état criblé (Fig. 3) also are listed in Table 2 (cases 4 and 7–9).

Discussion

Fisher [4, 6] clarified the clinical, pathologic, and epidemiologic features of lacunae. Also known as penetrating branch occlusions, lacunae are small infarcts lying in deeper noncortical parts of the cerebrum and brainstem. They are caused by occlusion of penetrating branches that arise from the middle cerebral, posterior cerebral, and basilar arteries, and less commonly from the anterior cerebral and vertebral arteries. The causes of the vascular occlusion are atheromata, lipohyalinosis, fibrinoid necrosis, and embolization [6, 10].

In about 90% of cases lacunar infarcts are associated with hypertension [4, 6]. In our series, five (83.3%) of the six cases (cases 2–6) with lacunae had clinical evidence of hypertension during life and/or pathologic evidence of concentric muscular hypertrophy of the left ventricle and severe systemic atherosclerosis at the time of postmortem examination. These five subjects were also elderly (Table 1). One subject with lacunae (case 1) had no history or pathologic evidence of hypertension, had minimal systemic atherosclerosis, and was 37 years old at the time of death. The patient's history was remarkable for IV drug abuse, and pathologic examination was notable for basilar meningitis. The mechanism of the multiple lacunae in this case presumably was caused by embolism to perforating branches or direct occlusion of these branches by the basilar meningitis.

In a review of 1042 brains from 1950 to 1954, Fisher [4] observed that one or more lacunae were found in 114 brains (11%). Sites of involvement were the lentiform nuclei (almost always the putamen) (37%), pons (16%), thalami (14%), caudate nuclei (10%), posterior limb of the internal capsule and corona radiata immediately above (10%), frontal lobe white matter anterolateral to the head of the caudate nucleus (4%), other sites of the supratentorial white matter (7%), and cerebellum (2%). Those in the cerebellum occurred close to the dentate nuclei or nearby in the middle cerebellar peduncle. In our series of 14 lacunar infarctions, eight (57%) were in the deep gray-matter nuclei (four [29%] in the putamen, two [14%] in the dentate nuclei, and two [14%] in the thalami), five (36%) were in the white matter, and one (7%) was in the brainstem.

Fisher [4, 6] observed that recent lacunae showed early or advanced liquefaction necrosis. In the chronic stage they showed an irregular cavity with a few strands of fine fibrillary connective tissue. Fatty macrophages were in the cavity, their number diminishing with the age of the lesion. The walls of the infarct comprised a dense fibroglial matting in which there were many plump astrocytes. In the gray matter lacunae often were linear, irregularly stellate, and collapsed, while in the white matter they more often maintained a round shape. In our cases the configuration was linear or ovoid in seven of

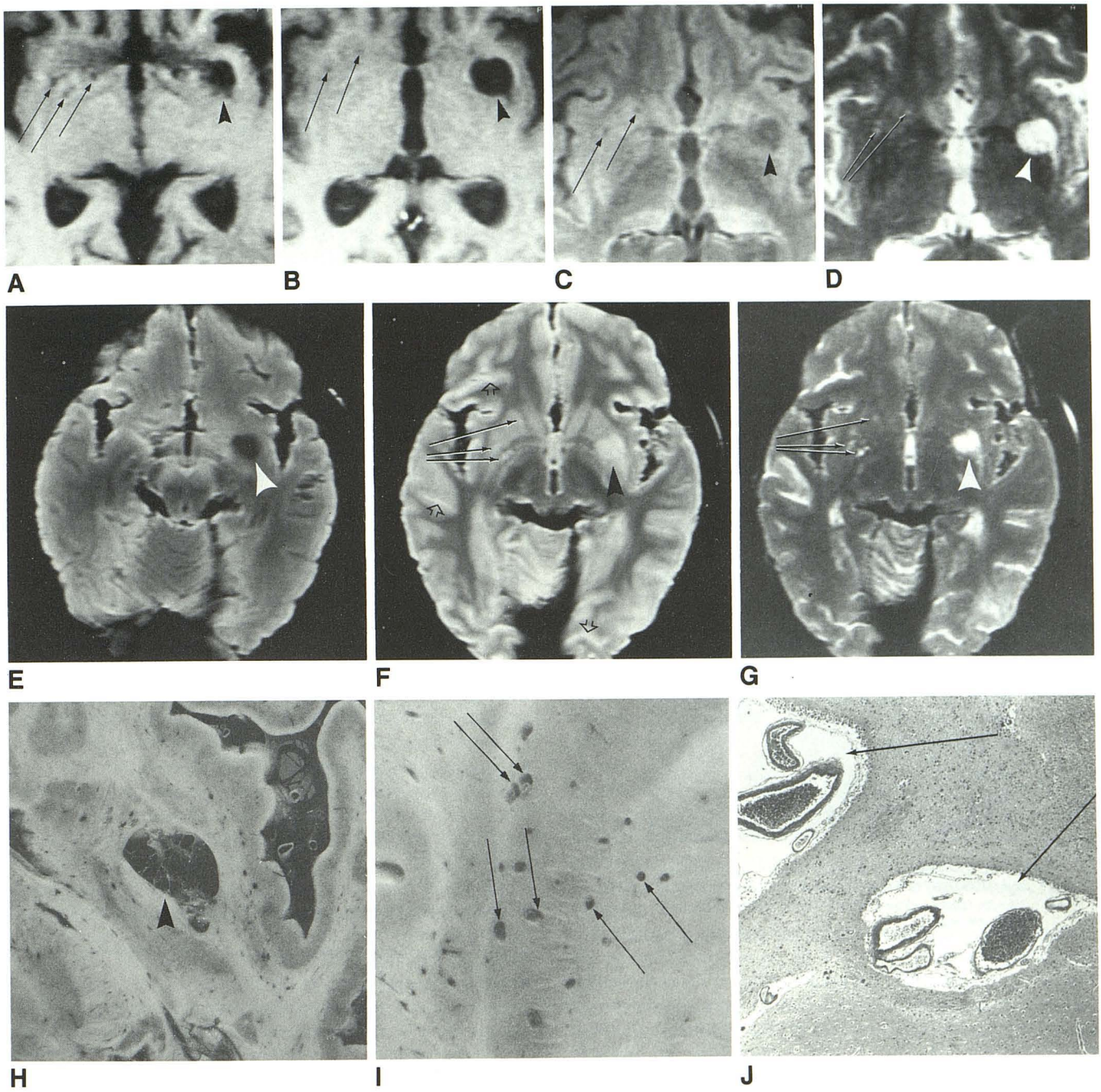

Fig. 3.—Case 4 (*A–I*): cystic lacunar infarct (*arrowheads*) in left putamen. Prominent perivascular spaces (*solid arrows*) in right putamen.

A–D, Axial MR images, 600/20 (*A* and *B*), 2500/30 (*C*), and 2500/80 (*D*) before death (×2 magnification). Dilated Virchow-Robin spaces are very small and either round or linear. Both this cystic infarct and état criblé are isointense relative to CSF on all three pulse sequences. On long TR/short TE sequence (*C*), cystic infarct, dilated perivascular spaces, and CSF are hypointense relative to gray matter and approximately isointense relative to white matter.

E–G, Axial MR images, 300/20 (*E*), 2500/30 (*F*), and 2500/80 (*G*), after death and subsequent formalin fixation (no magnification). There is no apparent change in morphology of infarct. Its contents are isointense relative to fluid in sulci. Perivascular spaces are slightly more pronounced on this nonmagnified MR scan in postfixation state. They are isointense relative to fluid in sulci. In contrast to in vivo MR, gray matter is hyperintense relative to white matter on short TR sequence (*E*). On the long TR/short TE sequence (*F*), cystic infarct, dilated perivascular spaces, and fluid in sulci (*open arrows*) are hyperintense relative to brain parenchyma (both gray and white matter).

H and *I*, Gross pathology. *H* shows cavitated, round infarct. Histopathology (not shown) revealed reactive astrocytes in the wall of this old healed infarct. *I* shows dilated perivascular spaces in putamen (slightly more prominent along lateral margin) and in internal capsule.

J, Stained section of basal forebrain of a different elderly patient with hypertension (case 7) illustrates degree of perivascular spaces (*arrows*) frequently occurring in these individuals. (H and E)

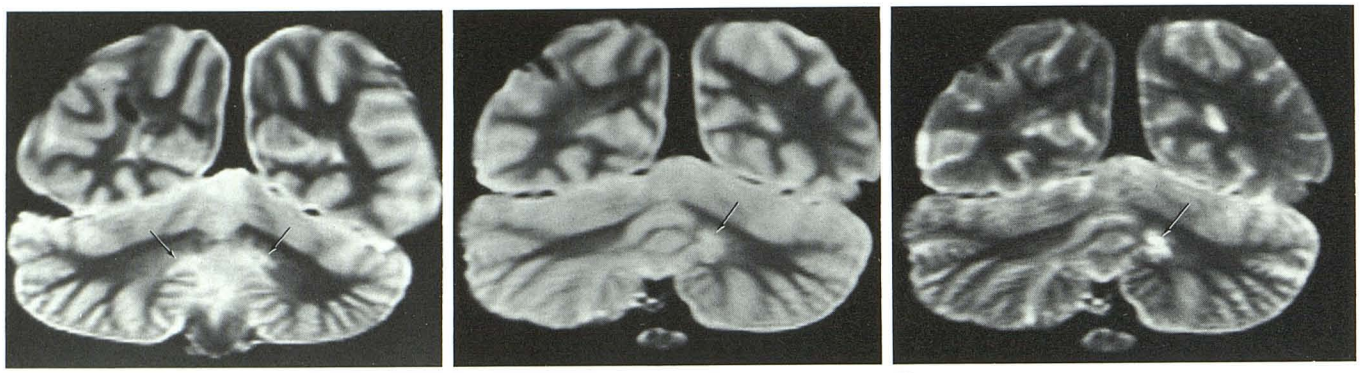

Fig. 4.—Case 1: bilateral dentate lacunae. Coronal MR images, 2500/30 (*A* and *B*) and 2500/80 (*C*), of brain specimen. Bilateral slitlike lesions (*arrows*), left greater than right, are hyperintense relative to brain parenchyma on both long TR sequences.

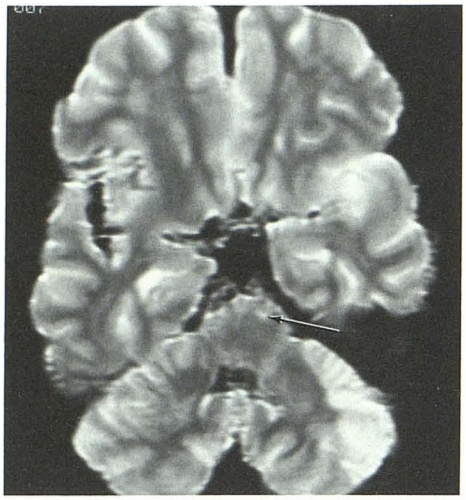

Fig. 5.—Case 3: brainstem lacuna. Axial MR image, 2500/30, of brain specimen. Lacuna is slitlike minute focus (*arrow*) hyperintense relative to brain parenchyma.

TABLE 2: MR Signal Intensities of Noncystic Lacunar Infarctions, État Criblé Without Surrounding Parenchymal Abnormalities, and Cystic Lacunar Infarctions

Lesions	Long TR/ Short TE	Long TR/ Long TE
Noncystic lacunar infarctions[a]:		
In vivo:		
Relative to brain	Hyperintense	Hyperintense
Relative to CSF	Hyperintense	Approximately isointense
Postmortem:		
Relative to brain	Hyperintense	Hyperintense
Relative to water-formalin solution	Slightly hyperintense to approximately isointense	Approximately isointense
État criblé[b] and cystic lacunar infarctions[c]:		
In vivo:		
Relative to brain	Hypointense	Hyperintense
Relative to CSF	Isointense	Isointense
Postmortem:		
Relative to brain	Hyperintense	Hyperintense
Relative to water-formalin solution	Isointense	Isointense

[a] Cases 1, 2, 3, 5, and 6.
[b] Cases 4, 7, 8, and 9.
[c] Case 4.

the eight affecting deep gray-matter nuclei (Figs. 1, 2, 4, and 5), round in one case affecting the putamen (Fig. 3), ovoid or slitlike in those affecting the white matter, and slitlike in the brainstem (Fig. 5).

Although lacunar infarctions usually are less than 1 cm in size, 17% of the cases in Fisher's series [4, 6] measured 1 cm or greater, in which case they were called giant lacunae (Fig. 3). In our series, 12 (86%) were less than 1 cm and two (14%) were 1 cm or greater in their greatest diameter (Table 1). Lacunae are defined as being caused by occlusion of penetrating vessels. Size is not a criterion. Alternatively, small infarctions, such as small watershed infarctions, may resemble lacunae morphologically, but they are not lacunae because they are not caused by branch occlusion of penetrating vessels.

All the lacunae in our series except one were hyperintense relative to brain parenchyma on long TR sequences (Figs. 1, 2, 4, and 5; Table 2), both in vivo and after formalin fixation. The single exception was in case 4 (Fig. 3). True cystic formation may occur in the chronic stages of infarction, and therefore the fluid may demonstrate signal characteristics identical to those of CSF in vivo [11] or to fluid in the subarachnoid space in the postmortem state on all pulse sequences (Table 2; Fig. 3). All pathologically verified lacunae were detected on MR. In those cases in which CT was performed, it disclosed the supratentorial infarcts but failed

to reveal the brainstem or dentate lacunae. The superiority of MR over CT in the evaluation of the posterior fossa has been described by previous investigators [12, 13].

In a study of the relative prevalence of état criblé, Cole and Yates [14] examined 100 brains of patients with hypertension and 100 cases from age- and gender-matched normotensives. The patients were 17–85 years old. They found dilatation of perivascular spaces in 38 of the 100 hypertensive subjects and in nine of the 100 normotensive patients. This occurred more often in elderly subjects. Similarly, all subjects in our study with dilated perivascular spaces were hypertensive and 50 years old or older (Table 1). Hughes [15] attributed the loosening of the adventitia of blood vessels from the surrounding brain tissue to spiraled elongations of small intracerebral arteries under the pulsations of raised blood pressure. Blackwood [3] suggested an alternative mechanism: First there is état pre-criblé, in which the myelin sheaths in the parenchyma surrounding the vessels are thin, pale, and sinuous. There is no associated dilatation of the perivascular space in this stage. Subsequently, rarefaction and disintegration of the perivascular parenchyma occur.

Cases 4 and 7 (Fig. 3) demonstrate the MR and pathologic features of état criblé in two patients with hypertension. The perivascular spaces demonstrated here most likely surround the lateral lenticulostriate arteries, branches of the middle cerebral artery. They number between six and eight, and the largest has a diameter of 250–400 μm. They run across the lateral surface of the putamen, parallel to the external capsule [16]. Other perforators that supply the putamen and internal capsule arise from the anterior cerebral (the recurrent artery of Heubner) and branches of the anterior choroidal artery.

On MR, état criblé areas in the basal ganglia are round or linear in shape, and are seen on successive axial sections beginning just above the level of the bifurcation of the internal carotid into the anterior and middle cerebral arteries through a variable thickness of the putamen (Fig. 3). Although there is some overlap in size, they are usually smaller than lacunae (Table 1). When they were characterized pathologically only by prominent Virchow-Robin spaces, they were isointense relative to CSF in vivo or to fluid in the subarachnoid space in the postmortem fixed state on all pulse sequences (Table 2). We did not observe pathologic changes in the parenchyma surrounding the dilated perivascular spaces. We can speculate that if there is adjacent gliosis and/or demyelination, this area would not be isointense relative to CSF on all pulse sequences on MR. Instead, it may be hyperintense relative to CSF and to brain parenchyma on the long TR/short TE sequence. This may be clarified further by additional studies.

All cases with pathologically verified prominent perivascular spaces were detected on MR. CT was performed in two cases and failed to reveal any corresponding abnormality.

Cases 1 and 4 allow us to compare the appearance on MR in vivo and postmortem after formalin fixation of brain parenchyma, lacunae, and prominent Virchow-Robin spaces (Figs. 1 and 3). After formalin fixation of the brain in case 4, gray matter was hyperintense relative to white matter on the short TR sequence (Fig. 3). This is different from an MR examination performed in a live subject, in which white matter is hyperintense relative to gray-matter on the short TR sequence. Unger et al. [17] described this same change after formalin fixation of brain specimens. They suggested that it possibly results from the more marked shortening of the T1 of gray matter than of white matter after formalin fixation as was described by Kamman et al. [18]. Thickman et al. [19] reported a rapid drop in the T1 values of rat liver and spleen after fixation with neutral buffered formalin owing to the loss of water by the fixation process.

The change in the orientation of the left putaminal lacunar infarct between the in vivo and postmortem MR studies of case 1 likely was from the decompression of the lateral ventricles (Fig. 1). At the time of the in vivo MR examination, a large arachnoid cyst obstructed the fourth ventricle with resultant hydrocephalus. This was surgically resected before death. There was no change in the morphology or intensity of the lacunar infarct relative to brain parenchyma on the long TR sequences.

CSF was hypointense relative to gray matter and approximately isointense relative to white matter on the long TR/short TE (2500/30) sequence (Figs. 1A and 3C). Water with dilute formalin was hyperintense relative to brain parenchyma (both gray and white matter) on this same pulse sequence (Figs. 1D and 3F). This relative change in signal intensity after fixation presumably was from a shortening of the T1 of water by formalin. This relative higher signal intensity on the long TR/short TE sequence must be considered when comparing brain parenchyma or variable lesions with water mixed with formalin before extrapolating to the live patient.

Case 4 also allowed us to evaluate état criblé with MR while the patient was living and after death and subsequent formalin fixation of the brain. Although the état criblé remained isointense relative to fluid in the subarachnoid space, these areas were slightly more prominent in number and size after fixation (Fig. 3). Greenfield [2] observed similar changes in paraffin sections but not in celloidin sections of brain, and he considered it to be from a shrinkage artifact in the former instance.

In summary, lacunae are small infarcts caused by penetrating branch occlusion [4, 6]. On MR, all were hyperintense relative to brain parenchyma on long TR sequences, except for one chronic infarct that underwent cystic change and was isointense relative to CSF in vivo or to fluid in the subarachnoid space in the postmortem state on all pulse sequences. Although one lacuna in the putamen was round, the usual morphology of lacunae was slitlike or ovoid. A spectrum of perivascular changes has been described as état criblé, which comprises dilated Virchow-Robin spaces with or without associated changes of gliosis and/or demyelination in the surrounding parenchyma [1–5]. They may occur in the basal ganglia and white matter. We have identified dilated Virchow-Robin spaces in the basal ganglia without accompanying changes in the surrounding parenchyma. On MR, in contrast to lacunae, dilated Virchow-Robin spaces usually were smaller round or linear foci, were isointense relative to CSF or to fluid in the subarachnoid space in the postmortem state on all pulse sequences, and were identified on successive axial sections along the course of the penetrating vessels.

MR studies of formalin-fixed brain specimens provide an opportunity to directly correlate MR findings with gross and microscopic pathology. However, changes caused by the fixation process must be considered before extrapolating to the MR examination of the brain in vivo.

ACKNOWLEDGMENT

We thank Pierre Rabischong for assistance in the preparation of this work.

REFERENCES

1. Greenfield JG. Infectious diseases of the central nervous system. In: Greenfield JG, Blackwood W, McMenemey WH, Meyer A, Norman RM, eds. *Neuropathology.* London: Edward Arnold, **1958**:132–229
2. Durand-Fardel M. *Traite du ramollissement du cerveau.* Paris: Balliere, **1843**
3. Blackwood W. Vascular diseases of the central nervous system. In: Greenfield JG, Blackwood W, McMenemey WH, Meyer A, Norman RM, eds. *Neuropathology* London: Edward Arnold, **1958**:67–131
4. Fisher CM. Lacunes: small, deep cerebral infarcts. *Neurology* **1965**;15:774–784
5. Brierly JB, Graham DI. Hypoxia and vascular disorders of the central nervous system. In: Adams JH, Corsellis JAN, Duchen LW, eds. *Greenfield's neuropathology*, 4th ed. New York: Wiley, **1984**:125–207
6. Fisher CM. Lacunar strokes and infarcts: a review. *Neurology* **1982**;32:871–876
7. Marie P. Des foyers lacunaires de desintegration et de differentsautres etats cavitaires du cerveau. *Rev Med* (Paris) **1901**;21:281
8. Awad IA, Johnson PC, Spetzler RF, Hodak JA. Incidental subcortical lesions identified on magnetic resonance imaging in the elderly. II. Post-mortem pathological correlations. *Stroke* **1986**;17:1090–1097
9. Braffman BH, Zimmerman RA, Trojanowski JQ, Gonatas NK, Hickey WF, Schlaepfer WW. Brain MR: pathologic correlation with gross and histopathology. 2. Hyperintense white-matter foci in the elderly. *AJNR* **1988**;9:629–636
10. Mohr JP. Lacunes. *Stroke* **1982**;13:3–11
11. Brant-Zawadzki M, Kucharczyk W. Vascular disease: ischemia. In: Brant-Zawadzki M, Norman D, eds. *Magnetic resonance imaging of the central nervous system.* New York: Raven, **1987**:221–234
12. Hans JS, Bonstelle CT, Kaufman B, et al. Magnetic resonance imaging in the evaluation of the brainstem. *Radiology* **1984**;150:705–712
13. Lee BCP, Kneeland JD, Deck MDF, et al. Posterior fossa lesions: magnetic resonance imaging. *Radiology* **1984**;153:137–143
14. Cole FM, Yates PO. Comparative incidence of cerebrovascular lesions in normotensive and hypertensive patients. *Neurology* **1968**;18:255–259
15. Hughes W. Origin of lacunes. *Lancet* **1965**;2:19–21
16. Salamon G, Huang YP. *Radiologic anatomy of the brain.* Berlin: Springer-Verlag, **1976**:195–209
17. Unger EC, Gado MH, Fulling KF, Littlefield JF. Acute cerebral infarction in monkeys: an experimental study using MR imaging. *Radiology* **1987**;162:789–795
18. Kamman RL, Go KG, Stomp GP, Hulstaert CE, Berendsen HJC. Changes of relaxation times T1 and T2 after biopsy and fixation. *Magn Reson Imaging* **1985**;3:245–250
19. Thickman DI, Kundel HL, Wolf G. Nuclear magnetic resonance characteristics of fresh and fixed tissue: the effect of elapsed time. *Radiology* **1983**;148:183–185